Chemical Kinetics of the NaO ($A\ ^2\Sigma^+$) + O(^{3}P) Reaction†

J. Griffin,‡ D. R. Worsnop,*,§ R. C. Brown,§ C. E. Kolb,*,§ and D. R. Herschbach*,‡

Department of Chemistry and Chemical Biology, Harvard University, Cambridge, Massachusetts 02138, and Center for Cloud and Aerosol Chemistry, Aerodyne Research, Inc., Billerica, Massachusetts 01821-3976

Received: July 25, 2000; In Final Form: October 17, 2000

Recent evidence has shown that the mesospheric sodium nightglow, a chemiluminescent process which produces atomic sodium D-line radiation in the Earth's upper atmosphere, proceeds through the first excited ($A\ ^2\Sigma^+$) electronic state of NaO. The rate of D-line radiation production is proportional to the rate constant for the reaction of NaO($A\ ^2\Sigma^+$) + O(^{3}P) and its branching ratio to produce excited Na(^{2}P) rather than ground-state Na(^{2}S). The only previously published measurement of the NaO + O(^{3}P) reaction rate and branching ratio was performed under slow flow conditions and almost certainly primarily represents the reaction of ground-state NaO ($X\ ^2\Pi$). We present low-pressure measurements of the NaO + O reaction kinetics using an NaO source reaction known to produce NaO in the ($A\ ^2\Sigma^+$) state and determine the 290 K reaction rate constant to be $(5.1 \pm 1.8) \times 10^{-10}$ cm^3 s^{-1} and the branching ratio to produce Na(^{2}P) to be 0.14 ± 0.04. New data on the termolecular rate coefficient for the reaction Na + O_2 + He → NaO_2 + He at 290 K are also presented.

Introduction

Atomic sodium ablated from meteorites entering the Earth's atmosphere forms the mesospheric sodium layer. This layer typically extends from ~80 to 100−110 km in altitude and peaks at concentrations of several thousand Na cm^{-3} near 90 km.[1] At night the layer can be observed to emit visible Na D-line radiation known as the sodium nightglow.[1,2] The accepted explanation for chemiluminescent production of the mesospheric sodium nightglow (reactions 1−3) was first published by Sydney Chapman in 1939:[3]

$$Na + O_3 \rightarrow NaO + O_2 \quad (1)$$

$$NaO + O \rightarrow Na(^2P) + O_2 \quad (2a)$$

$$\rightarrow Na\ (^2S) + O_2 \quad (2b)$$

$$Na(^2P) \rightarrow Na(^2S) + h\nu \quad (3)$$

The Chapman mechanism allows the potential chemical energy produced by solar induced photodissociation of upper atmospheric molecular oxygen, which is stored in the form of upper atmospheric O and O_3, to drive the chemiluminescent production of Na D-line radiation. Chapman later suggested that this mechanism could also account for the long-lived visible glow produced by the atmospheric entry of some larger meteors.[4] However, quantitative atmospheric models of this latter phenomenon failed to reproduce the magnitude of the radiation observed from large "meteor trails"[5] until Kolb and Elgin[6] pointed out that reactions 1 and 2 could be expected to proceed by electron jump mechanisms and would have rate constants near the gas kinetic limit, even at the very low temperatures (~200 K) of the upper mesosphere. Using rate constants estimated by Kolb and Elgin, atmospheric models were able to reproduce the approximate magnitude of both the normal sodium nightglow and long-lived "meteor trails".[1,6,7] Laboratory experiments eventually confirmed the magnitude of rate constants predicted by Kolb and Elgin for both reaction 1[8,9] and reaction 2.[9,10]

In 1980, on the basis of what was known about mesospheric levels of O_3 and typical sodium nightglow emission rates, Bates and Ojha[7] estimated that the product of the rate constant, k_1, for reaction 1 (which is rate controlling in the Chapman mechanism since upper mesospheric [O] ≫[O_3]), and the branching ratio, f_2, for reaction 2 to produce electronically excited Na(^{2}P) would need to be $k_1 f_2 > 1 \times 10^{-10}$ cm^3 s^{-1}. Bates and Ojha[7] also presented a symmetry correlation analysis of reaction 2 for ground-state NaO($X\ ^2\Pi$) reacting with O(^{3}P), which they claimed supported an f_2 as large as 0.33. In 1986, Swider[11] used somewhat updated atmospheric and kinetic data to determine that $k_1 f_2 > 2.1 \times 10^{-10}$ cm^3 s^{-1} was required. Using our measured k_1 of $(6.9 \pm 1.5) \times 10^{-10}$ cm^3 s^{-1} at 216 K,[8] Swider's analysis requires an $f_2 > 0.3$. More recent analyses based on atmospheric kinetic models plus measured Na layer intensities and Na D-line emissions by Plane and co-workers suggest that an $f_2 \sim 0.1$ is sufficient.[12,13]

Unfortunately, the only laboratory measurement of f_2, determined by Plane and Husain[10] in a relatively high pressure, slow flow heat pipe experiment, indicated that $f_2 \leq 0.01$. Since Plane and Husain used a slow flow reactor, with estimated NaO residence times before reaction of order 1 s, it is certain that they were predominantly studying NaO in its ground $X\ ^2\Pi$ state. While the interpretation of this experiment has been criticized by Schofield,[14,15] it is very unlikely that its estimate of f_2 is in error by an order of magnitude. However, in 1993 we reported a crossed molecular beam study of reaction 1 that showed its NaO product was produced predominantly, and quite possibly exclusively, in the low-lying $A\ ^2\Sigma^+$ state.[16] This conclusion was reinforced by photoelectron studies of the product of reaction 1 by Wright et al.[17] A symmetry correlation analysis of the NaO($A\ ^2\Sigma^+$) + O(^{3}P) reaction indicated that f_2 for this reaction along energetically assessable doublet surfaces could be as large

† Part of the special issue "Harold Johnston Festschrift".

* Corresponding authors: worsnop@aerodyne.com, kolb@aerodyne.com, fax: 978-663-4918; hbach@chemistry.harvard.edu, fax: 617-495-4723.

‡ Harvard University.

§ Aerodyne Research, Inc.

10.1021/jp002641m CCC: $20.00
Published on Web 12/21/2000

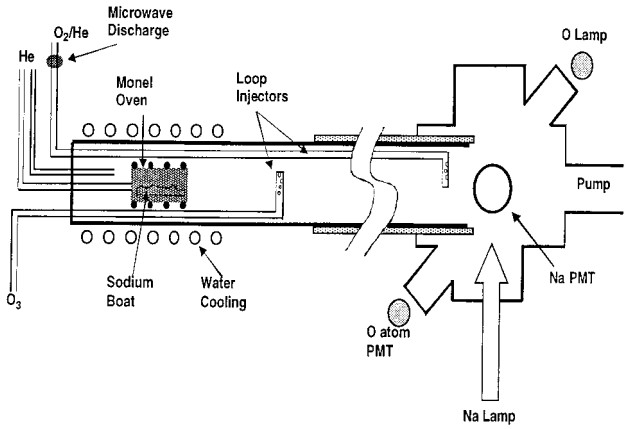

Figure 1. Schematic of the fast-flow reactor for $Na/O_3/O$ kinetics.

as 0.67,[18] while any correlation to excited Na(^{2}P) from the NaO(X $^2\Pi$) ground state is through energetically forbidden quartet states. Given this latter fact, the symmetry analysis presented by Bates and Ojha for the ground-state reaction[7] is not actually in conflict with the low value of f_2 measured for the NaO ground-state reaction.[10] Thus, our recent work,[16,18] supported by work in other laboratories,[10,17] strongly indicates that Chapman's simple mechanism expressed by reactions 1−3 must be amended so that it proceeds though the excited NaO(A $^2\Sigma^+$) state:

$$\mathrm{Na} + \mathrm{O_3} \xrightarrow{k_1} \mathrm{NaO(A\ ^2\Sigma^+)} + \mathrm{O_2} \qquad (1')$$

$$\mathrm{NaO(A\ ^2\Sigma^+)} + \mathrm{O} \xrightarrow{k_{2'a}} \mathrm{Na(^2P)} + \mathrm{O_2} \qquad (2'a)$$

$$\xrightarrow{k_{2'b}} \mathrm{Na(^2S)} + \mathrm{O_2} \qquad (2'b)$$

$$\mathrm{Na(^2P)} \xrightarrow{k_3} \mathrm{Na(^2S)} + h\nu \qquad (3)$$

Further, since our symmetry/reaction energy analysis[18] suggests that $f_2 \sim 0$ for the NaO(X $^2\Pi$) ground state, any loss of the NaO(A $^2\Sigma^+$) produced by reaction 1′ by either radiative or collisional quenching before it can react with O will be manifested by an apparent reduction in f_2.

Until recently, the NaO(A $^2\Sigma^+$) state had not been observed experimentally but had been widely investigated theoretically.[19] We recently observed over 150 lines of the A $^2\Sigma^+ \leftarrow$ X $^2\pi$ infrared transition and determined that $T_{0-0} = 1992.905$ cm^{-1} for this transition.[20] In this paper we report on experiments to investigate the room temperature kinetics of reaction 2 under low-pressure conditions using reaction 1 as the source of NaO. The goal of this work was to assess the overall rate constant, $k_{2'}$, and the branching ratio, $f_{2'} = k_{2'a}/(k_{2'a} + k_{2'b})$, for reaction 2 with NaO(A $^2\Sigma^+$) as the predominant reactant under conditions where radiative and/or collisional quenching losses of NaO(A $^2\Sigma^+$) are minimized.

Experimental Design and Procedures

The apparatus used for this study is a 3.8 cm diameter fast-flow reactor designed for alkali atom and molecule kinetics studies, as shown schematically in Figure 1. Its basic features have been described previously[8] and will only be summarized here. The first 20 cm section of the flow reactor contained a monel sodium oven and was water cooled. Na atoms were generated by heating ∼1 g samples of metallic sodium in a silver "boat" placed in the 2.5 cm oven to temperatures commensurate with Na vapor pressures of 10^{-5} to 10^{-3} Torr, producing initial [Na] in the flow reactor on the order of 10^{12} to 10^{13} cm^{-3}. The Na vapor was entrained in a small He flow and introduced into the main (usually He) carrier gas flow. The main, 70 cm long, reaction section of the flow reactor can be uniformly cooled to 215 K, but was operated at ∼290 K for the studies reported here. Gas volumetric flows were monitored with a calibrated thermal conductivity mass flow meter, and pressures were determined with a MKS Baratron (Model 122A) capacitance manometer. Total flow reactor pressure varied from 1.4 to 4.3 Torr for the results reported below.

Two 0.6 cm o.d. glass tubes served as movable injectors for introducing O_3 and atomic O flows into the reactor. A hexagonal Teflon cap with holes through each of its six radial faces was fitted to the atomic O injector to speed mixing with the main flow. Commercial chemicals including 99.95% sodium metal (Alfa), 99.995% gaseous He, 99% gaseous N_2O, 99.993% gaseous O_2, and 99.999% gaseous Ar were used without further purification. The method of O_3 generation, introduction, and quantification has been described previously.[8,21] Atomic O was generated in an Evenson cavity microwave discharge through a He/O_2 mixture. The discharge tube was fused into the inlet of the second injector and the discharge cavity translated with the injector along a guide rail parallel to the flow reactor. A combination of two three-way solenoid valves created a computer controlled four-way valve which allowed rapid switching of carefully matched gas flows between the injectors and the main flow reactor. This allowed the rapid on/off switching of gaseous reactants on time scales that are short compared with output drifts in atomic Na from the oven.

The reaction section of the flow reactor projects into a 10 cm diameter six-way cross whose four sidearms perpendicular to the flow reactor permit optical detection of reactant and product species. Ground-state atomic Na(^{2}S) was detected via an Na hollow cathode lamp resonance fluorescence, while excited-state Na(^{2}P) was detected using the same photomultiplier tube (PMT) detector by monitoring lamp-shuttered chemiluminescent emission. A computer controlled spring-loaded solenoid shutter masked the Na lamp during the chemiluminescence measurements. Atomic oxygen was monitored via resonance absorption with a PMT detector using the O (^{3}S−^{3}P) triplet at 130.22, 130.49, and 130.60 nm following the method of Anderson.[22] The atomic O discharge lamp was operated to produce optically thin emissions. It consisted of a 1.2 cm He filled (to ∼5 Torr) glass tube with a MgF_2 window fused to one end. The lamp was excited with ∼30 W from an Evenson microwave discharge cavity. Powered metallic Ba in one sidearm served as an internal getter for the lamp assembly, while $KMnO_4$ in a second sidearm served as an oxygen source. Atomic O(^{3}P) levels of $(2-9) \times 10^{12}$ were measured in the flow reactor, dependent on discharge conditions, injector position, and sodium oxide levels.

A DT2805 Data Translation board allowed personal computer control of reactant line solenoid valves and the Na lamp shutter and also collected data from the Baratron and the Na and O phtomultiplier tube detectors. Typical experimental runs yielded data from a range of predetermined conditions for each injector position. Selected conditions included O discharge source flow, O_3 flow, main carrier flow, and Na lamp shutter position. Solenoid mechanical lags and flow times to clear injectors set minimum times required to reach steady-state conditions and allow transient free data collection. In general time the times required to reach stable flow conditions and acquire sufficient data ranged from 5 to 30 s.

Typical kinetic runs were made under a range of variable flows through the first and second injectors, using the resonance fluorescence determination of ground-state [Na] as a function of the second injector position as the common observable. Four of the most important flow conditions are described here. First, [Na] without the O_2/He discharge on and with He/Ar rather than He/O_3 flowing through the first injector was determined. Here Na loss is due only to the relatively slow Na + O_2 + M → NaO_2 + M reaction and Na loss to the flow reactor walls. Second, the O_2/He discharge was ignited, producing atomic O and a small, but significant, amount of O_3 from O + O_2 + M. Atomic O levels were monitored by resonance absorption. Here, Na loss is dominated by NaO formation from reaction 1′ and by termolecular recombination of Na with O to form NaO. NaO formation is not completely balanced by Na re-formation via reaction 2/2′ and can be followed by secondary reaction 4a between NaO + O_3:

$$\mathrm{NaO} + \mathrm{O_3} \rightarrow \mathrm{NaO_2} + \mathrm{O_2} \qquad (4a)$$

$$\rightarrow \mathrm{Na} + 2\mathrm{O_2} \qquad (4b)$$

The third experimental condition is similar to the second; O_2 is introduced through the first injector, enhancing [Na] loss due to the Na + O_2 + He reaction. In condition 4, O_3 in an He carrier is introduced though the first injector, converting most of the Na to NaO($A\ ^2\Sigma^+$) via reaction 1′, while the products O + O_3 of the O_2/He discharge continue to be added through the second injector. In this case, reactions 2′ and 4b continue to regenerate Na, but reaction 1′ also continues to consume it. Under this condition chemiluminescence from Na(^{2}P), created by reaction 2′a, is monitored via its emission, as well as the Na(^{2}S) from reactions 2′b, 3, and 4b.

In all four cases, there will be loss of sodium species, including Na, NaO, and NaO_2, on the flow reactor walls. Our previous work has shown that the loss of all Na species occurs at essentially unit probability with each wall collision and the rate of wall collisions can be well-estimated from calculated diffusion coefficients.[8,21] Experimental data on relative ground-state Na concentrations, for reaction conditions 1−4, atomic O concentrations, for reaction conditions 2 and 3, and Na chemiluminescent D-line emission levels, for reaction condition 3, were taken for a range of flow tube pressures between 1.4 and 4.3 Torr under room temperature conditions, 290 ± 2 K. In some runs N_2O, expected to be an effective quenchant for NaO($A\ ^2\Sigma^+$), since its ν_3 vibrational band is nearly coincident with T_{0-0} for the NaO A←X transition,[20] was added to the carrier flow, with little effect.

Results

The goal of this study was to investigate the magnitude of the overall rate coefficient for reaction 2′, $k_{2'} = k_{2'a} + k_{2'b}$, and the branching ratio for excited-state Na(^{2}P) production, $f_{2'} = k_{2'a}/(k_{2'a} + k_{2'b})$, under conditions where NaO is produced by reaction 1, and is predominantly NaO($A\ ^2\Sigma^+$). Since the data reported here were taken at flow reactor pressure below 5 Torr to minimize collisional quenching of NaO($A\ ^2\Sigma^+$), and since our spectroscopic measurements and available theoretical calculations indicate that the radiative lifetime of NaO($A\ ^2\Sigma^+$), 1−100 ms,[19,20] will be much longer than the chemical lifetime of NaO via reaction 2 of ∼0.25 ms under our experimental conditions, we believe that the $k_{2'}$ and $f_{2'}$ values reported below are representative of NaO in the $A\ ^2\Sigma^+$ state. The fact that even moderate amounts of added N_2O did not significantly diminish the observed Na(^{2}P) emission is taken as evidence that its collisional quenching by the He carrier flow is not a significant loss process under the low-pressure, fast-flow conditions employed for the kinetic measurements described below.

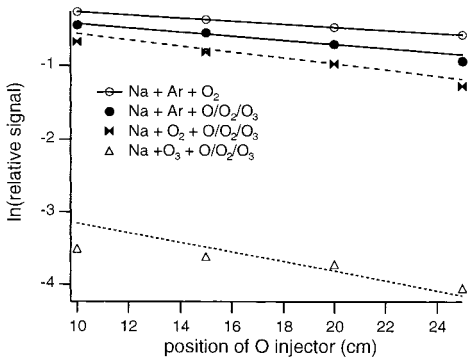

Figure 2. Experimental plots of [Na] decays and kinetic model fits for a 290 K, 4.3 Torr case. Reaction conditions corresponding to each data curve are explained in the text.

Representative experimental data taken at a flow reactor total pressure of 4.26 Torr and temperature of 290 K are shown in Figure 2. The top data points (open circles) are for experimental condition 1 and represent the Na decay as a function of second injector position with only Ar from the first injector and a He/O_2 mixture entrained from the second injector. The second highest data set (condition 2, filled circles) represent Ar flow through the first injector and an He/O_2 discharge on flow through the second injector, which provides a modest amount of O_3 from O + O_2 combination plus a high level of O. The third data set (condition 3, bowties) represents O_2 flow through the first injector and the same He/O_2 discharge on through the second injector as condition 2. The lowest data set (triangles) represents condition 4, with $[O_3] = 1.5 \times 10^{12}$ cm^{-3} added through the first injector and the He/O_2 discharge on with its O/O_2/O_3 mixture added though the second injector.

The data in Figure 2 have been simulated using a kinetic model based on the CHEMKIN code[23] and the reaction set shown in Table 1. Reaction rate coefficients for most sodium, sodium oxide, and oxygen species were adopted from the DeMore et al. evaluation of atmospheric reaction kinetic parameters,[24] although reaction rates for several termolecular (He third body) oxygen atom reactions were selected from the National Institute of Standards and Technology (NIST) kinetic data compilation.[25] A room temperature Na + O + He termolecular rate constant of 2.0×10^{-30} cm^6 s^{-1} was estimated from the Na + O_2 + He rate coefficient. These reactions proceed by an electron jump from the Na to the electrophilic reactant, followed by a Columbic attraction between the resulting Na^+ and O^- or O_2^-. Since the electron affinity of O (1.46 eV) is higher than that of O_2 (0.45 eV), the initial electron jump will occur at longer range, but the nascent NaO will also have a shorter lifetime against dissociation than the nascent NaO_2 while waiting for a third body collision to stabilize the reaction product. Our estimate that the Na + O + He reaction should be modestly faster than the Na + O_2 + He reaction is supported by a reported estimate of a 290 K rate for the Na + OH + He rate constant of $(4.1 \pm 0.9) \times 10^{-30}$ cm^6 s^{-1} (OH has an electron affinity of 1.83 eV), based on a measured value at 635 K extrapolated with a Tröe unimolecular reaction formulation to lower temperatures.[26] The estimate for the reaction rate coefficient for the NaO_3 + O reaction was taken from ref 12.

To ensure the current fast-flow reactor yielded reliable reaction rates, we fitted the measured [Na] decay rates for six 290 K experimental runs where O_2 was added through either

TABLE 1: Kinetic Mechanism Used in Fitting the NaO + O Reaction Rate Data

reaction	rate constant	source
	Wall-Loss Reactions	
$Na \rightarrow Na(s)$	$83.7\ s^{-1}$	modeled from diffusion coefficients
$NaO \rightarrow NaO(s)$	$139.3\ s^{-1}$	modeled from diffusion coefficients
$NaO_2 \rightarrow NaO_2(s)$	$69.7\ s^{-1}$	modeled from diffusion coefficients
$NaO_3 \rightarrow NaO_3(s)$	$63.5\ s^{-1}$	modeled from diffusion coefficients
$O \rightarrow O(s)$	$2.7\ s^{-1}$	modeled from diffusion coefficients
	Reactions from Chapman's Mechanism	
$Na+O_3 = NaO + O_2$	$1.0 \times 10^{-9}\ e^{-95/T}\ cm^3\ s^{-1}$	ref 24
$NaO + O = Na + O_2$	$(5.1 \pm 1.8) \times 10^{-10}\ cm^3\ s^{-1}$	see text
	Significant Secondary Reactions	
$Na + O + He = NaO + He$	$7.5 \times 10^{-29}\ cm^6\ s^{-1}$	estd—see text
$Na + O_2 + He = NaO_2 + He$	$(1.49 \pm 0.3) \times 10^{-30}\ cm^6\ s^{-1}$	see text
$NaO_2 + O = NaO + O_2$	$2.2 \times 10^{-11}\ cm^3\ s^{-1}$	ref 24
$NaO + O_3 = Na + O_2 + O_2$	$6.0 \times 10^{-11}\ cm^3\ s^{-1}$	ref 24
$NaO + O_3 = NaO_2 + O_2$	$1.1 \times 10^{-9}\ e^{-570/T}\ cm^3\ s^{-1}$	ref 24
$NaO_3 + O = NaO_2 + O_2$	$1.8 \times 10^{-11}\ T^{0.5}\ cm^3\ s^{-1}$	ref 12
$NaO + O_2 + He = NaO_3 + He$	$1.3 \times 10^{-30}\ cm^3\ s^{-1}$	ref 25
$O + O_3 = O_2 + O_2$	$8.0 \times 10^{-12}\ e^{-2060.0/T}\ cm^3\ s^{-1}$	ref 24
$O_2 + O + He = O_3 + He$	$3.5 \times 10^{-34}\ cm^6\ s^{-1}$	ref 25
$O + O + He = O_2 + He$	$1.3 \times 10^{-33}\ cm^6\ s^{-1}$	ref 25

TABLE 2: Na + O_2 + He → NaO_2 + He Kinetics Results (290 K)

run no.	k_5 ($cm^6\ s^{-1}$)
1	1.53×10^{-30}
2	1.34×10^{-30}
3	1.87×10^{-30}
4	1.53×10^{-30}
5	1.25×10^{-30}
6	1.43×10^{-30}
av	1.49×10^{-30}
std dev	0.30×10^{-30}

the first or second injector (condition 1). These decays are dominated by the termolecular reaction:

$$Na + O_2 + He \xrightarrow{k_5} NaO_2 + He \qquad (5)$$

Including computed diffusional wall loss for Na and NaO_2, the linear least-squares fits for k_5 from these six decays are tabulated in Table 2. The average of these data yields $k_5(290\ K) = (1.49 \pm 0.30) \times 10^{-30}\ cm^6\ s^{-1}$, where the stated error is one standard deviation about the mean. This result is in excellent agreement with the value of $(1.44 \pm 0.20) \times 10^{-30}\ cm^6\ s^{-1}$ for 290 K previously measured in our laboratory,[27] and in reasonable agreement with higher temperature values reported by Husain and Plane[28] ($(0.6 \pm 0.1) \times 10^{-30}\ cm^6\ s^{-1}$ for 724−844 K) and Vinckler et al.[29] ($(0.89 \pm 0.07) \times 10^{-30}\ cm^6\ s^{-1}$ for 290 K via a Tröe extrapolation of data taken between 392 and 777 K) and a single lower temperature point of $(1.2 \pm 0.2) \times 10^{-30}\ cm^6\ s^{-1}$ at 250 K reported by Plane and Rajeskhar.[30] We used the k_5 measured in this study in the CHEMKIN model.

Linear least-squares model fits to two condition 2 decays (filled circles), two condition three decays (bowties), and two condition 3 decays (triangles) with $k_{2'}$ as a free parameter yielded values of this rate coefficient where the A $^2\Sigma^+$ state is the predominant form of NaO. These individual fitted values of $k_{2'}$ are tabulated in Table 3. The mean value for the six fits of $k_{2'}$ at 290 K is $(5.1 \pm 0.8) \times 10^{-10}\ cm^3\ s^{-1}$, where the stated error is one standard deviation about the mean. In addition to the random measurement error expressed as the single standard deviation about the mean, it is prudent to add an estimate of the probable systematic errors involved in both measuring experimental variables and modeling the flow reactor kinetics to derive $k_{2'}$ Given the moderately indirect nature of the measurement, a prudent estimate of the additional uncertainty due to systematic error is ±20% of the measured value, leading to a final value of $k_{2'} = (5.1 \pm 1.8) \times 10^{-10}\ cm^3\ s^{-1}$ at 290 K.

TABLE 3: NaO + O → Na + O_2 Kinetics Results and Measured $f_{2'}$

NaO + O → Na + O_2 Kinetics Results (290 K)

run no.	$k_{2'}$ ($cm^3\ s^{-1}$)	run no.	$k_{2'}$ ($cm^3\ s^{-1}$)
1	5.71×10^{-10}	4	5.15×10^{-10}
2	5.98×10^{-10}	5	3.82×10^{-10}
3	5.81×10^{-10}	6	3.99×10^{-10}
av	5.08×10^{-10}	std dev	0.80×10^{-10}

Measured 290 K $f_{2'}$ Values[a]

	for given P (Torr)			
reac distance (cm)	4.3	4.3	3.2	1.4
10	0.149	0.142	0.137	0.122
15	0.137	0.139	0.125	0.131
20	0.123	0.124	0.112	0.106
25	0.083	0.092	0.080	0.077

[a] 16 pt av = 0.12; 16 pt std dev = 0.02; 8 initial pt av = 0.14; 8 initial point std dev = 0.01.

The solid lines plotted on the representative decay data shown in Figure 2 are simulations based on the average values derived for k_5 and $k_{2'}$. Fits to decays where these parameters were variables reproduced the decay curves more closely and yielded the individual run values tabulated in Tables 2 and 3.

A study state analysis for Na(^{2}P) from reaction 2′ and 3 yields

$$f_{2'}k_{2'}[NaO][O] = k_3[Na(^2P)] \qquad (6)$$

which can be rearranged to

$$f_{2'} = k_3[Na(^2P)]/k_{2'}[NaO][O] \qquad (7)$$

where k_3 is the inverse of the [Na(^{2}P)] radiative lifetime, $(16.40 \pm 0.03) \times 10^{-9}$ s.[31] In principle, we can determine [Na(^{2}P)] from its observed chemiluminescent signal (CL) in the reaction region in front of the Na PMT:

$$CL = (CV)(DE)k_3[Na(^2P)] \qquad (8)$$

where CV is the chemiluminescent photon optical collection volume for the Na PMT and DE is its detection efficiency. In

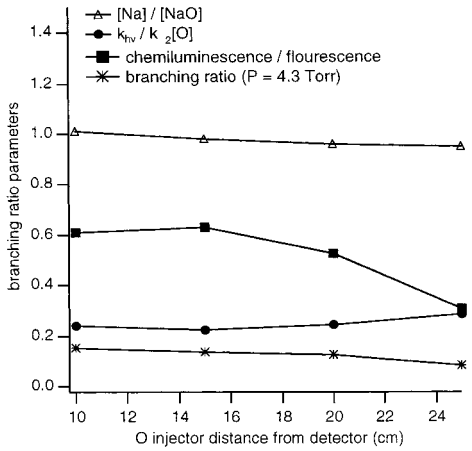

Figure 3. Plots of components of eq 11 and the resultant value of $f_{2'}$ as a function of reaction distance for a 290 K, 4.3 Torr case.

practice, it is more accurate to ratio out the optical collection and PMT efficiency factors by stimulating the ground-state Na(^{2}S) to fluorescence using the Na resonance lamp. Since the Na PMT optics were arranged so that the resonance lamp output fills the Na PMT field of view, with the lamp on the Na PMT records a signal which is the sum of CL plus a fluorescence signal equal to

$$\mathrm{FL} = (\mathrm{CV})(\mathrm{DE})k_{hv}[\mathrm{Na}] \tag{9}$$

where $k_{hv} = \sigma F/(1 + \alpha^2)^{1/2}$, σ is the Na(^{2}S$\rightarrow^2$P) absorption cross-section of 1.85×10^{-11} cm^2 derived from the excited-state radiative lifetime,[31] F is the measured resonance lamp photon flux though the PMT observation volume, and α is the overlap integral between the room temperature ground-state Na absorption line and the lamp output spectra.[2] The value of α can be obtained from the ratio of the Doppler broadened half-width of the lamp Na emission line and the room temperature Doppler broadened absorption width of the Na in the low-pressure flow reactor, which can be approximated by the square root of the ratio of the lamp operating temperature (600 K) divided by the flow tube gas temperature (290 K), to give $\alpha = 1.44$.

Combing eqs 8 and 9 yields

$$[\mathrm{Na}(^2\mathrm{P})] = (\mathrm{CL}/\mathrm{FL})k_{hv}[\mathrm{Na}]/k_3 \tag{10}$$

Substituting eq 10 into eq 7, the branching ratio, $f_{2'}$, to produce Na(^{2}P) can be derived from the expression

$$f_{2'} = (\mathrm{CL}/\mathrm{FL})(k_{hv}/k_{2'}[\mathrm{O}])([\mathrm{Na}]/[\mathrm{NaO}]) \tag{11}$$

where CL is the chemiluminescent signal from Na(^{2}P) and FL is the fluorescence signal in the same reaction volume from Na(^{2}S) (obtained by subtracting the chemiluminescence signal with the resonance lamp off from the total fluorescence plus chemiluminescence signal obtained with the Na lamp on). The ratio [Na]/[NaO] is taken from the kinetic model, and [O] is derived from the resonance absorption measurement.

Figure 3 shows the three terms in parentheses on the right-hand side of eq 5 for the data presented in Figure 2, as well as the resulting values of $f_{2'}$, all plotted as a function of the second injector's distance from the detection region. Table 3 displays the $f_{2'}$ values measured for four cases, with the total flow tube pressures on 4.2 (two cases) 3.2, and 1.4 Torr, respectively. For each case an $f_{2'}$ is determined for four reaction distances varying between 10 and 24 cm. Clearly, while the two shortest reaction distances in each case produce similar values, the measured $f_{2'}$ values are noticeably smaller for the two longer reaction distances. This is likely due to the influence of secondary chemistry, which is not completely accounted for by the reaction set in Table 1. The average and standard deviation of all tabulated 16 points are 0.12 ± 0.02, while the average and standard deviation for the two shortest reaction distance points are 0.14 ± 0.01. The average of the first two points is recommended as a more reliable value for $f_{2'}$. However, a significant allowance for systematic error must be added to the statistical error represented by the single standard deviation about this mean. Systematic uncertainties include the effect any NaO produced which is not in the $A\ \Sigma^+$ state (particularly from the Na + O + M and NaO_2 + O reactions), any loss of Na A state due to radiative, reactive (other than reaction 2′), or physical quenching, and systematic errors in the measured experimental and modeled parameters in eq 11, including uncertainty in the estimate of the spectral line shape overlap integral, α, and in the measurement of [O]. We estimate that these systematic errors combined with the computed statistical error result in a recommended value of $f_{2'} = 0.14 \pm 0.04$.

Discussion

The value of $k_{2'}$ (290 K) reported here, for conditions where the $A\ ^2\Sigma^+$ state is designed to be nearly the exclusive form of NaO, can be compared with the value of $(3.7 \pm 0.9) \times 10^{-10}$ cm^3 s^{-1} at 573 K obtained by Plane and Husain under conditions where NaO($X\ ^2\Pi$) predominated,[10] and the value of 1.6×10^{-10} cm^3 s^{-1} predicted for ground-state NaO($X\ ^2\Pi$) by a simple electron jump mechanism at mesospheric temperatures.[6] Obviously the two experimental values agree within their experimental errors. The reaction rate of O(^{3}P) with the ground state of NaO is ~3.8 eV exothermic, based on recently published ab initio calculations of D_o(NaO X) = 2.43 eV.[33] It seems reasonable to assume that the additional 0.16 eV of exothemicity for the $A\ ^2\Sigma^+$ state will not greatly influence the kinetics. We might expect a slightly longer range electron jump given the slightly lower ionization potential of NaO($A\ ^2\Sigma^+$). The evaluation of DeMore et al.[23] recommends a temperature independent value for k_2 of 3.7×10^{-10} cm^3 s^{-1}, while a temperature dependent rate coefficient which corresponds to a 300 K value of 2.7×10^{-10} cm^3 s^{-1} has been adopted by Plane and co-workers for atmospheric modeling.[12,13] Under conditions where NaO($A\ ^2\Sigma^+$) dominates, these values should be increased in future models.

The measured value of $f_{2'} = 0.14 \pm 0.04$ far exceeds the value of ~0.01 for the slow flow study of Plane and Husain,[10] which is presumably representative of the f_2 for NaO($X\ ^2$P). It is reasonably close to the value of ~0.1 derived by Plane and co-workers from model analyses of Na nightglow and associated atmospheric measurements[12,13] and is also comfortably below the upper limit of 0.67 we deduced from an analysis of symmetry correlations.[18]

Atmospheric Implications

It is critical that the excited-state kinetics (reactions 1′ and 2′) be considered in nightglow analyses similar to those of Plane and collaborators.[12,13] A recent publication by Hecht et al.[33] which used measured Na layer parameters from the Coqui Dos campaign to estimate f_2 is almost certainly in serious error because it was performed under very cold mesospheric conditions where the average O density was about 2×10^{11} cm^3. This means that the mean chemical lifetime of NaO($A\ ^2\Sigma^+$) created in reaction 1′ was $1/(k_{2'}[\mathrm{O}]) \sim 10$ ms. Langhoff[19] has calculated that the NaO($A\ ^2\Sigma^+, v'=0$) radiative lifetime is 14.5

ms and the calculated radiative lifetimes for higher upper vibrational states, which are surely populated given the exothermicity of reaction 2′, decrease rapidly and monotonically, e.g. 7.9 ms for $v' = 1$, 5.3 ms for $v' = 2$, 3.9 ms for $v' = 3$, to 1.4 ms for $v' = 9$. Therefore, if these calculated radiative lifetimes are at all accurate, it is very likely that the radiative loss of NaO(A $^2\Sigma^+$) exceeded its loss via reaction 2′. Since we know that ground-state NaO(X $^2\Pi$) + O does not produce Na(^{2}P) at significant levels,[10,16] radiative decay of NaO(A $^2\Sigma^+$) almost certainly helped produce the low estimate of f_2 (<0.05) Hecht et al. reported. Also at low rates of reaction 2′, NaO(A $^2\Sigma^+$) may be lost to physical quenching via collisions with N_2 and O_2 and by reactive collisions with H_2 and H_2O, all processes which Hecht et al. failed to consider. It is interesting to note that the similar analysis by Clemesha et al.[13] measured their highest Na levels near 98 km, where O atom densities were derived to be $\sim 8 \times 10^{11}$, allowing reaction 2′ to process a much higher fraction of the NaO(A $^2\Sigma^+$) produced by reaction 1′ and leading to a significantly higher estimate for f_2.

To perform the analyses presented in refs 13, 33, and 34 (where f_2 was varied over a large range) correctly, our value of $f_{2'}$ should be redetermined at typical mesospheric temperatures (180−220 K), although we do not expect the branching ratio for this exothermic reaction to depend strongly on temperature. In addition, rate coefficients for the reaction of NaO(A $^2\Sigma^+$) with H_2, H_2O, and O and its physical quenching rate constants by N_2 and O_2 should be measured over a significant temperature range extending down to mesospheric temperatures. Finally, accurate measurement of the NaO(A $^2\Sigma S^+ \rightarrow$ X ^{2}P) radiative lifetime as a function of v' as well as the nascent NaO(A $^2\Sigma^+$) vibrational distribution from reaction 1 also need to be made.

We believe the value of $f_{2'}$ for the NaO(A $^2\Sigma^+$) might be more precisely determined at various temperatures by exploiting our recent measurement of precise line positions for NaO(A $^2\Sigma^+ \leftarrow$ X ^{2}P) transition,[20] which should allow easier preparation of NaO(A $^2\Sigma^+$) using pulsed infrared laser techniques. More definitive values of $k_{2'}$, $f_{2'}$, and the rate coefficients for NaO(A $^2\Sigma^+$) physical, reactive, and radiative quenching at mesospheric temperatures should also be accessible using this technique. These parameters would then allow accurate nighttime upper mesospheric ozone profiles to be derived from the measurement of altitude resolved resonant fluorescent measurement of Na concentration profiles and Na D-line nightglow levels.[13,33,34]

Acknowledgment. We dedicate this paper to Professor Harold S. Johnston in celebration of his 80th birthday. In richly fulfilling his roles of mentor, teacher, textbook author, researcher, environmental leader, and gentleman, Hal Jonhston has inspired us. His life and work stand as an outstanding example of the power and purpose of physical chemistry in the twentieth century. We also thank Aerodyne colleagues M. S. Zahniser, D. D. Nelson, J. T. Jayne, S. Kallelis, and J. T. Mulholland for technical assistance and R. Heroux, E. Weinstock, and J. G. Anderson of Harvard for providing atomic oxygen resonance absorption equipment and advice. We also gratefully acknowledge the financial support of the Atmospheric Sciences Division of the National Science Foundation under Grant No. 9304528.

References and Notes

(1) Plane, J. M. C. *Intl. Rev. Phys. Chem.* **1991**, *10*, 55.
(2) Kolb, C. E.; Worsnop, D. R.; Zahniser, M. S.; Robinson, G. N.; Shi, X.; Herschbach, D. R. In *Gas-Phase Metal Reactions*; Fontijn, A., Ed.; Elsevier Science: Amsterdam, 1992; p 15.
(3) Chapman, S. *Astrophys. J.* **1939**, *90*, 309.
(4) Chapman, S. In *The Airglow and Aurorae*; Armstrong, E. B., Delgarno, A., Eds.; Pergammon Press: London, 1956; p 204.
(5) Baggaley, W. J. *Nature* **1975**, *257*, 567.
(6) Kolb, C. E.; Elgin, J. B. *Nature* **1976**, *263*, 488.
(7) Bates, D. R.; Ojha, P. C. *Nature* **1980**, *286*, 790.
(8) Worsnop, D. R.; Zahniser, M. S.; Kolb, C. E. *J. Phys. Chem.* **1991**, *95*, 3691 (errata, *J. Phys. Chem.* **1992**, *96*, 9088) and references cited therein.
(9) Plane, J. M. C.; Helmer, H. In *Research in Chemical Kinetics;* Compton, R. G., Hancock, G., Eds.; Elsevier Science: Amsterdam, 1994; Vol. 2, p 313.
(10) Plane, J. M. C.; Husain, D. *J. Chem. Soc., Faraday Trans. 2* **1986**, *82*, 2047.
(11) Swider, W. *J. Geophys. Res.* **1986**, *91*, 4067.
(12) Helmer, M.; Plane, J. M. C. *J. Geophys. Res.* **1993**, *98*, 23207.
(13) Clemesha, B. R.; Simonich, D. M.; Takahashi, H.; Melo, S. M. L.; Plane, J. M. C. *J. Geophys. Res.* **1995**, *100*, 18909.
(14) Schofield, K. *Geophys. Res. Lett.* **1993**, *20*, 2837.
(15) Schofield, K. *Int. J. Chem. Kinet.* **1993**, *25*, 719.
(16) Shi, X.; Herschbach, D. R.; Worsnop, D. R.; Kolb, C. E. *J. Phys. Chem.* **1993**, *97*, 2113.
(17) Wright, T. G.; Ellis, A. M.; Dyke, J. M. *J. Chem. Phys.* **1993**, *98*, 2891.
(18) Herschbach, D. R.; Kolb, C. E.; Worsnop; Shi, X. *Nature* **1992**, *356*, 414.
(19) Langhoff, S. R.; Partridge, H.; Bauschlicher, C. W., Jr. *Chem. Phys.* **1991**, *153*, 1, and references cited therein. Calculated NaO (A $^2\Sigma^+$) radiative lifetimes for various vibrational levels were supplied by: Langhoff, S. R. Private communication, 1992.
(20) Joo, S.; Worsnop, D. R.; Kolb, C. E.; Kim, S. K.; Herschbach, D. R. *J. Phys. Chem. A.* **1999**, *103*, 3193.
(21) Silver, J. A.; Kolb, C. E. *J. Phys. Chem.* **1986**, *90*, 3263.
(22) Anderson, J. G. *Geophys. Res. Lett.* **1975**, *2*, 231.
(23) Kee, R. J.; Miller, J. H.; Jefferson, T. H. *CHEMKIN: A Chemical Kinetics Code Package*; Sandia Laboratories: Albuquerque, NM, 1989.
(24) DeMore, W. B.; Sander, S. P.; Golden, D. M.; Hampson, R. F.; Kurylo; M. J.; Howard, C. J.; Ravishankara, A. R.; Kolb, C. E.; Molina, M. J. *Chemical Kinetics and Photochemical Data for Use in Stratospheric Modeling*; Report No. JPL 97-4; Jet Propulsion Laboratory: Pasadena, CA, 1997.
(25) Mallard, W. G.; Westley, F.; Herron, J. J.; Hampson, R. F. *NIST Chemical Kinetics Database−Version 6.01*; Standard Reference Data Center, National Institute of Standards and Technology: Gaithersburg, MD, 1994.
(26) Husain, D.; Plane, J. M. C.; Xiang, C. C. *J. Chem. Soc., Faraday Trans. 2* **1984**, *80*, 1619.
(27) Silver, J. A.; Zahniser, M. S.; Stanton, A. C.; Kolb, C. E. *Proceedings of the Twentieth Symposium (International) on Combustion*; The Combustion Institute: Pittsburgh, PA, 1984; p 605.
(28) Husain, D.; Plane, J. M. C. *J. Chem. Soc., Faraday Trans. 2* **1984**, *78*, 163.
(29) Vinckler, C.; Dumoulin, A.; De Jaegere, S. *J. Chem. Soc., Faraday Trans.* **1991**, *87*, 1075.
(30) Plane, J. M. C.; Rajasekhar, B. *J. Phys. Chem.* **1991**, *93*, 3135.
(31) Gaupp, A.; Kuske, P.; Andrä, H. J. *Phys. Rev. A* **1982**, *26*, 3351.
(32) Lee, E. P. F.; Wright, T. G.; Dyke, J. M. *Mol. Phys.* **1992**, *77*, 501.
(33) Hecht, J. H.; Collins, S.; Kruschwitz, C.; Kelly, M. C.; Roble, R. G.; Walterscheid, R. L. *Geophys. Res. Lett.* **2000**, *27*, 453.
(34) Takahashi, H.; Melo, S. M. L.; Clemesha, B. R.; Simonich, D. M.; Stegman, J.; Witt, G. *J. Geophys. Res.* **1996**, *101*, 4033.